On the Multi-spacecraft Determination of Periodic Surface Wave Phase Speeds and Wavelengths

Foullon et al. 2010, Journal of Geophysical Research doi: 10.1029/2009JA015189

C. Foullon[1], C.J. Farrugia[2], A.N. Fazakerley[3], C.J. Owen[3], F.T. Gratton[4], R.B. Torbert[2]

[1] Univ. Warwick, UK, [2] SSC/UNH, USA, [3] MSSL/UCL, UK, [4] IFP, Argentina

CFSA and astrophysics centre for fusion, space

THE UNIVERSITY OF WARWICK

Introduction

Observations of surface waves on the magnetopause indicate a wide range of phase velocities and wavelengths.

- Periods in the Pc5 (1-10mHz) range
- Phase velocities: 60 - 350 km/s
- Wavelengths λ: from 2 to a few tens of R_E

Wave characteristics, such as the sizes of KH vortices, and other derived quantities may be of physical importance, notably via comparison with theoretical and numerical models, to elucidate

- the conditions leading to the waves' formation,
- their possible non-linear development
- and their role in the plasma entry to the magnetosphere.

Thus, reliable estimates of the wave characteristics are important.

Non-linear effects have been invoked to account for

(i) Wavelengths of a few R_E , much longer than predicted by linear theory *[Belmont & Chanteur, 1989]*

(ii) Tailward steepening of the KH leading fronts observed with Cluster *[Owen et al., 2004; Foullon et al., 2008]*, consistent with the growing phases of KH waves *[De Keyser et al., 2005]*

(iii) Presence of vortices, a phenomenon supported by the interpretation of data in single and multi-s/c analyses *[Hones et al., 1981; Saunders et al., 1983; Fairfield et al., 2000; Hasegawa et al., 2004; Fairfield et al. 2007]*

(iv) Inverse dependence between IMF CA and λ *[Foullon et al., 2008]*, which confirms the significance of source regions and non-linear development.

Key factor: λ-stretching effect with distance of the observing site from the subsolar point.

- stream of flow velocity: magnetosheath flow picks up
- the magnetic field strength decreases, implying that all gyroradii increase.

Linear MHD, in the long wavelength limit or no layer [e.g. Chandrasekhar, 1961, Hasegawa, 1975]

$$v_p = \frac{N_1(kV_1) + N_2(kV_2)}{k(N_1 + N_2)} \qquad v_g = \frac{\partial\omega}{\partial k} = \frac{N_1V_1 + N_2V_2}{N_1 + N_2}$$

Phase speed *Group velocity*

Other factors may control λ:

(i) Thickness of the boundary layer *[e.g. Walker, 1981; Miura & Pritchett, 1982]*

(ii) Non-linear development of dominant structures *[e.g. Belmont & Chanteur, 1989; Miura, 1999a, b]*

(iii) The global magnetospheric geometry of unstable source regions controlled by the IMF orientation *[e.g. Farrugia et al., 1998; Foullon et al., 2008]*

Despite those latest theoretical developments, most observational as well as theoretical works, assume some 'flow approximations', which may be seen to correspond to limiting cases to v_g.

1. Surface Wave Phase Speeds from Multi-spacecraft Observations

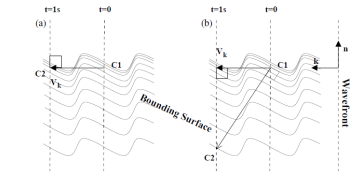

Figure 1. Surface wave propagating in the k direction with phase speed, V_k, showing bounding surfaces sampled by spacecraft C1 at time t=0 and C2 at t=1s, respectively, (a) without and (b) with inclination of the two-spacecraft direction with respect to k.

Timelags between two or more spacecraft can give a qualitative upper estimate to the phase speed.

In the case of surface waves, the timings obtained locate the same phase in the waveform, but not necessarily for the same iso-surface (or discontinuity).

The application of 4-s/c timing analysis in this case thus differs from the case of shocks, where the propagation along the normal can be expected.

The 2-point and 4-point measurements have the same problem of the apparent speed. V_p is obtained by 'deprojection' along the wave propagation direction.

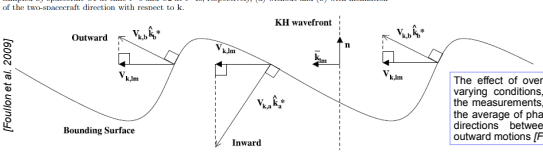

[Foullon et al. 2009]

The effect of overall motions in response to varying conditions, which may interfere with the measurements, can be mitigated by taking the average of phase speeds and propagation directions between pairs of inward and outward motions *[Foullon et al. 2008]*.

Schematic waveform of a KH wave propagating in the $\hat{k}_{hn}$ direction (to the left), showing the relationship between the phase speed, $V_{k,hn}$, and the velocities $V_{k,n}$ and $V_{k,h}$ measured in the directions $\hat{\mathbf{k}}_n$ and $\hat{\mathbf{k}}_h$, respectively, normal to a pair of bounding surfaces. The star symbol indicates that the values are projected in the ($\hat{k}_{hn}$, n) plane. $V_{k,n}$ and $V_{k,h}$ are apparent speeds along the surface normals.

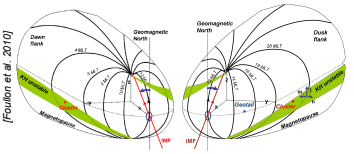

[Foullon et al. 2010]

Triangulation or 4-s/c timing analysis has been applied in two Cluster studies of surface waves, that by Owen et al. [2004] and that by Foullon et al. [2008], on the dawn and dusk flanks respectively. Further comparisons in Foullon et al. [2010].

Multi-spacecraft analysis allows a more precise determination of wave characteristics than ever before and reveal shortcomings of approximations to the phase speed, that take a predetermined fraction of the magnetosheath speed *[e.g. V_s / 2, Chen et al. 1993]*, or the average flow velocity in the boundary layer.

Both Cluster studies indicate phase speeds (V_p=50-90 km/s) and wavelengths (λ= 2-3.4 Re) in the lower range compared to other reports in the same locales.

- With the magnetosheoath flow speed V_s~260 km/s, V_p~ V_s / 3.
- The average flow velocity in the boundary layer along X_{GSM} of 212 km/s (Hasegawa, 2009) is twice as large as the phase speed deprojected along X_{GSM} of 100 km/s. On the Cluster 2000 km scale size, this discrepancy can only lead to a spatial or temporal shift correction between time series of (2000x (1/100-1/212)~) **11 s** at most << period of 215 s. This gives an apparent good alignment but an **inaccuracy of λ by a factor greater than 2!**

2. Wavelength Proxy from Two-point Distant Comparison

Using two-point distant magnetic field observations and spectral analysis of the tailward magnetic field component, we propose an alternative method to estimate the wavelength and phase speed at a single spacecraft from a statistical fit to the data at the other site.

Method

Magnetic wave activity is characterised with the largest component B(m) of the magnetic field; amplitude variations in this tailward component (m pointing sunward on the dusk flank) relate to λ changes (due to stretching in the wave propagation direction).

Using the spectral power as proxy for λ, we can infer the relation between the two parameters at Cluster and apply this relation to obtain the λ at Geotail.

A statistical fit can be obtained at Cluster thanks to the various levels of IMF CA, which control λ.

Amplitude variations in Bm are assumed to depend on λ, whatever the nature and origin of the perturbations, so that the wave activities from sites, which are not necessarily aligned in a given propagation path can still be compared.

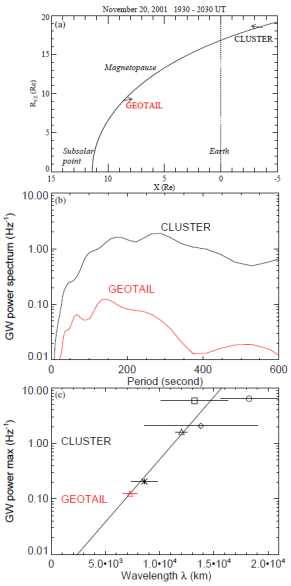

Figure 4. 2001 November 20 event. (a) Orbit view of *Geotail* on the dayside and *Cluster* tailward in a radial cross-section of the dusk magnetosphere. (b) Global wavelet power spectra for the detrended and normalised time series $\delta B(m)/|B|$ at *Cluster* (black) and *Geotail* (red). (c) Global wavelet maximum power in the range 100-250 s (4-10 mHz), versus the wavelengths. See text for details.

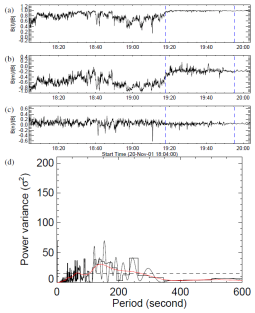

Figure 2. Magnetic wave activity at *Geotail* in the interval between 18:04 and 20:04 UT on November 20, 2001. (a-c) Normalised magnetic field time series $\delta(|B|)/|B|$, projected into a *lmn*-coordinate system: a trend is overlaid on the m-component, $B(m)/|B|$. Vertical dashed lines mark interval in the boundary layer. (d) Lomb-Scargle periodogram (thin solid), normalised Fourier power spectrum (histogram mode) and normalised global wavelet spectrum (thick red) on the detrended time series $\delta(B(m)/|B|)$. The horizontal dashed line is the 95% confidence level for the periodogram.

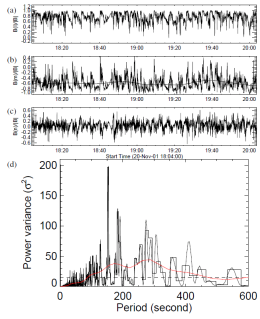

Figure 3. Magnetic wave activity at *Cluster* C2 in the same interval and same format as in Figure 2.

Results

The best fit to the data points at Cluster, using the linear relation

$$\lambda(P_{GW}) = \lambda_0 + A\log(P_{GW})$$

with λ in km and P_{GW} in Hz^{-1}, is obtained for λ_0 =11860 ± 471 km and A = 1739 ± 487 km.

This relation is used to estimate λ at Geotail= 7253 ± 690 km.

From the dominant spectral period (144.2s) we infer a propagation speed of the perturbations at Geotail of **50 ± 5 km/s**. This value is slightly lower but close to the average ion velocity projected in the m-direction, 57 km/s in absolute value. **This indicates that the perturbations at Geotail are likely to be advected with the local flow.** The value obtained is much lower than the 115 km/s estimate given by *Hasegawa et al. [2009]* (based on flow approximations).

This method might be further validated with more observations.

Email: claire.foullon@warwick.ac.uk

With thanks to: PIs from CLUSTER and GEOTAIL

Science & Technology Facilities Council

References:

Belmont and Chanteur (1989), Phys. Scr. 40, 124
Chandrasekhar (1961), Hydrodyanmic and Hydromagnetic Stability (Clarendon: Oxford)
Chen et al. (1993), GRL 20, 2699
De Keyser et al. (2005), Space Sci. Rev. 118, 231
Fairfield et al. (2000), JGR 105, 21159
Fairfield et al. (2007), JGR 112, A8206
Farrugia et al. (1998), JGR 103, 6703
Foullon et al. (2008), JGR 113,A11203
Foullon et al. (2009), JGR 114, A10201
Foullon et al. (2010), AIPCP 1216, 483
Hasegawa (1975), Plasma Instabilities and Nonlinear Effects (Springer Verlag)
Hasegawa et al. (2004), Nature 430, 755
Hasegawa et al. (2009), JGR 114, A12207
Hones et al. (1981), JGR 86, 814
Miura (1999a), GRL 26, 409
Miura (1999b), JGR 104, 395
Miura and Pritchett (1982), JGR 87, 7431
Saunders et al. (1983), Planet. Space Sci. 31, 1099
Owen et al. (2004), Ann. Geophys. 22, 971
Walker (1981), Planet Space Sci. 29, 1119